

Rapid-Process Nucleosynthesis in Neutrino-Magneto-Centrifugally Driven Winds

Shigehiro NAGATAKI¹ and Kazunori KOHRI²

¹ *Department of Physics, School of Science, the University of Tokyo, 7-3-1 Hongo, Bunkyo-ku, Tokyo 113-0033*

E-mail(TY): nagataki@utap.phys.s.u-tokyo.ac.jp

² *Yukawa Institute for Theoretical Physics, Kyoto University, Kyoto, 606-8502, Japan*

(Received ; accepted)

Abstract

We have studied whether the rotation and magnetic fields in neutrino-driven winds can be key processes for the rapid-process (r-process) nucleosynthesis. We have examined the features of a steady and subsonic wind solutions which extend the model of Weber and Davis (1967), which is a representative solar wind model. As a result, we found that the entropy per baryon becomes lower and the dynamical timescale becomes longer as the angular velocity becomes higher. These results are inappropriate for the production of the r-process nuclei. As for the effects of magnetic fields, we found that a solution as a steady wind from the surface of the proto-neutron star can not be obtained when the strength of the magnetic field becomes $\geq 10^{11}$ G. Since the magnetic field in normal pulsars is of order 10^{12} G, a steady wind solution might not be realized there, which means that the models in this study may not be adopted for normal proto-neutron stars. In this situation, we have little choice but to conclude that it is difficult to realize a successful r-process nucleosynthesis in the wind models in this framework.

Key words: nucleosynthesis, abundances — stars: magnetic fields — stars: rotation — supernovae: general

1. Introduction

It is one of the most important astrophysical problems that the sites where the rapid-process (r-process) nucleosynthesis occurs are not still known exactly. There are, at least, three reasons that make the study on r-process nucleosynthesis important. One of them is a very pure scientific interest. The mass numbers of the products of r-process nucleosynthesis are very high ($A = 80\text{--}250$), which means that the most massive nuclei in the universe are synthesized through the r-process. You can guess easily that the situation in which the r-process nuclei are synthesized is a very peculiar one in the universe. We want to know where, when, and how the r-process nuclei are formed. Second reason is that some r-process nuclei can be used as chronometers. For example, the half-lives of ^{232}Th and ^{238}U are 1.405×10^{10} yr and 4.468×10^9 yr, respectively. Therefore, if we can predict the mass-spectrum of the products of r-process nucleosynthesis precisely, we can estimate the ages of metal-poor objects which contain the r-process nuclei by observing its abundance ratio. Third reason is that some r-process nuclei can be used as tools of the study on the chemical evolution in our Galaxy (e.g., Ishimaru and Wanaajo 1999), which has a potential to reveal the history of the evolution of our Galaxy itself. Due to the reasons mentioned above, the study on the r-process nucleosynthesis is very important.

The conditions in which the r-process nucleosynthesis occurs successfully are (e.g., Hoffman et al. 1997): (i) neutron-rich ($n_n \geq 10^{20} \text{ cm}^{-3}$), (ii) high entropy per baryon, (iii) small dynamical timescale, and (iv) small Y_e . This is because r-process nuclei are synthesized through the non-equilibrium process of the rapid neutron capture on the seed nuclei that is synthesized through the alpha-rich freezeout (e.g., Hoffman et al. 1997). In other words, an explosive and neutron-rich site with high entropy will be a candidate for the location where the r-process nucleosynthesis occurs.

The candidates of the reliable sites are collapse-driven supernovae (e.g., Woosley et al. 1994) and/or neutron star mergers (e.g., Freiburghaus et al. 1999). This is because these candidates are thought to have a potential to satisfy the conditions mentioned above. However, we think that the collapse-driven supernovae are thought to be more probable sites than the neutron star mergers, because metal poor stars already contain the r-process nuclei (e.g., Freiburghaus et al. 1999). In fact, McWilliam et al. (1995) reported that the abundance of Eu can be estimated in 11 stars out of 33 metal-poor stars. These observations prove that r-process nuclei are produced from the early stage of the star formation in our Galaxy. Comparing the event rate of collapse-driven supernovae ($10^{-2} \text{ yr}^{-1} \text{ Gal}^{-1}$; van den Bergh and Tammann 1991) with the neutron star merger ($10^{-5} \text{ yr}^{-1} \text{ Gal}^{-1}$; van den Heuvel and Lorimer 1996; Bethe and Brown 1998), we can see that collapse-driven supernovae are favored since they can supply the

r-process nuclei from the early stage of the star formation in our Galaxy. Also, Cowan et al (1999) reported that the abundance ratio of r-process nuclei in metal poor stars are very similar to that in the solar system. This proves that r-process nuclei are synthesized through the similar conditions. This will be translated that, at least, most of the r-process nuclei are from one candidate. Therefore, we assume in this paper that most of the r-process nuclei are synthesized in the collapse-driven supernovae.

There are many excellent and precise analytic and/or numerical computations on the r-process nucleosynthesis in the collapse-driven supernovae. However, so far it seems that there is no report that the r-process nuclei can be reproduced completely. For example, Takahashi et al. (1994) performed numerical simulations assuming Newtonian gravity and reported that entropy per baryon in the hot bubble is about 5 times smaller than the required value. Qian and Woosley (1996; hereafter QW96) also reported analytic treatments of the neutrino-driven winds from the surface of the proto-neutron star. At the same time, their analytical treatments are tested and confirmed by numerical methods. However, it was shown that the entropy derived by their wind solutions fall short, by a factor of 2–3, of the value required to produce a strong r-process (Hoffman et al. 1997). In order to solve this difficulty, Qian and Woosley (1996) included a first post-Newtonian correction to the equation of the gravitational force. As a result, they reported that the entropy increases and the dynamical timescale is reduced by a factor of ~ 2 . Cardall and Fuller (1997) developed this argument by considering a fully general relativistic treatment. They showed that a more compact neutron star leads to higher entropy and a shorter dynamical timescale in the neutrino-driven wind. In order to confirm their conclusion quantitatively, Otsuki et al. (2000) have surveyed the effects of general relativity parametrically. They reported that r-process can occur in the strong neutrino-driven winds ($L_\nu \sim 10^{52}$ erg s $^{-1}$) as long as a massive ($\sim 2.0 M_\odot$) and compact (~ 10 km) proto-neutron star is formed. It is very interesting because such a solution can not be found in the frame work of Newtonian gravity (Qian and Woosley 1996). Such a solution is confirmed by the excellent numerical calculations (Sumiyoshi et al. 1999). However, the equation of state (EOS) of the nuclear matter has to be very soft to achieve such conditions. Although a few non-standard models of EOS can satisfy them (Wiringa et al. 1988) as long as the matter is sufficiently cold, it seems to be very difficult to achieve them in the phase of the proto-neutron star. In fact, the r-process nuclei can not be produced in the numerical simulations with a normal EOS (Sumiyoshi et al. 1999). Thus, it seems that the difficulty can not be solved by only the effects of general relativity.

There is only one report that r-process nucleosynthesis occurred successfully. That is the work done by Woosley

et al (1994; here after WWMHM94). In their numerical simulation, the entropy per baryon becomes higher and higher as the computation time goes on. Finally, at very late phase of neutrino-driven wind (~ 10 s after the core-collapse), successful r-process occurs. However, there are some problems in their results. First of all, it is unclear why the entropy per baryon at the late phase becomes so high as their results. In fact, when we adopt the analytic formulation of QW96, such a high entropy should not be obtained. Although the general relativistic effects are included in WWMHM94, such a high entropy could not be obtained in Otsuki et al (2000). Therefore, the discrepancy between WWMHM94 and QW96 can not be simply explained by only the general relativistic effects. Also, WWMHM94 has a problem that much nuclei whose mass numbers are ~ 90 are produced in the early stage of the neutrino-driven winds. To agree with the observational solar system abundances, we have to abandon the products at the early stage of the neutrino-driven winds. In addition, the successful mass-spectrum at the late phase of neutrino-driven winds would be destroyed when the reactions of neutral-current neutrino spallations of nucleons from ${}^4\text{He}$ are taken into consideration (Meyer 1995). They reported that the entropy should be increased by (30–50)% in order to restore the $A = 195$ peak. They are extremely large modifications to the model. Although WWMHM94 is surely the very remarkable and interesting work, the problem of r-process nucleosynthesis has not been solved completely.

Due to the reason mentioned above, it will be natural to think that there may be an (some) effect(s) that will help the r-process nucleosynthesis. In this study, we investigate the effects of rotation and magnetic fields on the synthesis of the r-process nuclei. In general, it is difficult to study their effects since the system including them is complicated and numerical simulations are needed in order to investigate them precisely. Since there is no numerical simulation like that, our final goal is to perform such realistic numerical simulations. However, as stated above, to perform such a numerical simulation will be a heavy task. Even if we can do it in future, it will be difficult to explain the results without any simple analytical studies. In this situation, before performing such numerical simulations, we examine the physical conditions of simple, exact, and steady solutions of the neutrino-driven wind including the effects of rotation and magnetic fields. We use the model that is the extension of the solution presented by Weber and Davis (1967), which is used as a representative model for the solar wind. In this study, we add the effects of neutrino heating and cooling to the solution and examine whether the effects of rotation and magnetic fields can help the synthesis of r-process nuclei.

In section 2., we explain the formulation for the wind in the hot bubble. Results are shown in section 3.. Summary

and discussions are presented in section 4..

2. Formulations

2.1. Basic Equations

In Gaussian units, the Euler equation acted on by electromagnetic forces can be written as (Shapiro and Teukolsky 1983)

$$\frac{d\vec{v}}{dt} = -\frac{1}{\rho}\nabla P - \nabla\Phi - \frac{1}{8\pi\rho}\nabla B^2 + \frac{1}{4\pi\rho}(\vec{B} \cdot \nabla)\vec{B}. \quad (1)$$

Here

$$\frac{d}{dt} = \frac{\partial}{\partial t} + \vec{v} \cdot \nabla \quad (2)$$

is the Lagrangian time derivative following a fluid element.

In this paper, we study a steady flow which has ϕ -symmetry around the equatorial plane of the proto-neutron star. Thus, we use the spherical coordinate (r, θ, ϕ) for convenience. The origin $r=0$ is set at the center of the proto-neutron star. In this coordinate, the Euler equation in the radial direction for the system that has ϕ -symmetry can be written as

$$v_r \frac{dv_r}{dr} = -\frac{1}{\rho} \frac{dP}{dr} - \frac{GM}{r^2} - \frac{v_\theta}{r} \frac{\partial v_r}{\partial \theta} + \frac{v_\theta^2 + v_\phi^2}{r} - \frac{B_\phi}{4\pi\rho r} \frac{\partial}{\partial r}(rB_\phi) - \frac{B_\theta}{4\pi\rho r} \left[\frac{\partial}{\partial r}(B_\theta r) - \frac{\partial B_r}{\partial \theta} \right]. \quad (3)$$

Here we used the conservation of mass:

$$\frac{1}{r^2} \frac{\partial}{\partial r}(r^2 \rho v_r) + \frac{1}{r \sin \theta} \frac{\partial}{\partial \theta}(\rho v_\theta \sin \theta) = 0. \quad (4)$$

The equation for the evolution of material energy, ϵ , is

$$\rho \dot{q} = \nabla \cdot (\rho \epsilon \vec{v}) + P \nabla \cdot \vec{v} \quad (5)$$

$$= \left(\frac{1}{r^2} \frac{\partial}{\partial r}(r^2 \rho \epsilon v_r) + \frac{1}{r \sin \theta} \frac{\partial}{\partial \theta}(\rho \epsilon v_\theta \sin \theta) \right) + P \left(\frac{1}{r^2} \frac{\partial}{\partial r}(r^2 v_r) + \frac{1}{r \sin \theta} \frac{\partial}{\partial \theta}(v_\theta \sin \theta) \right) \quad (6)$$

where \dot{q} is the net specific heating rate due to neutrino interactions (Qian and Woosley 1996). In this study, we consider three neutrino heating and/or cooling processes (neutrino absorption on free nucleons, neutrino scattering processes on the electrons and positrons, and electron and positron capture on free nucleons) as

$$\dot{q} = \dot{q}_{\nu N} + \dot{q}_{\nu e} - \dot{q}_{e N}, \quad (7)$$

where

$$\dot{q}_{\nu N} = 1.55 \times 10^{-5} N_A [(1 - Y_e)L_{\nu_e, 51} \epsilon_{\nu_e, \text{MeV}}^2 + Y_e L_{\bar{\nu}_e, 51} \epsilon_{\bar{\nu}_e, \text{MeV}}^2] \frac{1-x}{R_6^2} \quad [\text{erg s}^{-1} \text{ g}^{-1}], \quad (8)$$

$$\dot{q}_{\nu e} = 3.48 \times 10^{-6} N_A \frac{T_{\text{MeV}}^4}{\rho_8} \left(L_{\nu_e, 51} \epsilon_{\nu_e, \text{MeV}} + L_{\bar{\nu}_e, 51} \epsilon_{\bar{\nu}_e, \text{MeV}} + \frac{6}{7} L_{\nu_\nu, 51} \epsilon_{\nu_\nu, \text{MeV}} \right) \frac{1-x}{R_6^2} \quad [\text{erg s}^{-1} \text{ g}^{-1}], \quad (9)$$

and

$$\dot{q}_{eN} = 3.63 \times 10^{-6} N_A T_{\text{MeV}}^6 \quad [\text{erg s}^{-1} \text{ g}^{-1}]. \quad (10)$$

Here R_6 is the neutrino sphere radius in units of 10^6 cm, ρ_8 is the density in units of 10^8 g cm $^{-3}$, T_{MeV} is the temperature in units of 1 MeV, $x = (1 - R^2/z^2)^{1/2}$, N_A is Avogadro number, $L_{\nu, 51}$ is the individual neutrino luminosity in 10^{51} erg s $^{-1}$, $\epsilon_{\nu, \text{MeV}}$ is an appropriate neutrino energy ϵ_ν in MeV (Qian and Woosley 1996). In this study, we set $\dot{q}=0$ at $T \leq 0.5$ MeV, because free nucleons are bound into α -particles and heavier nuclei and electron-positron pairs annihilate into photons.

The pressure P and internal energy ϵ are determined approximately by the relativistic electrons and positrons and photon radiation as long as $T \geq 0.5$ MeV. Then, the pressure and internal energy can be written as

$$P = \frac{11\pi^2}{180} \frac{k^4 T^4}{\hbar^3 c^3} \quad [\text{dyn cm}^{-2}] \quad (11)$$

and

$$\epsilon = \frac{11\pi^2}{60} \frac{k^4 T^4}{\hbar^3 c^3 \rho} \quad [\text{erg g}^{-1}], \quad (12)$$

where k and \hbar are Boltzmann and Planck constants, respectively. These are the basic equations in this paper. Precisely, although we might have to consider the effects of annihilation of electron-positron pairs on the dynamics at $T \leq 0.5$ MeV, the effects seems to be little (Sumiyoshi et al. 1999).

2.2. Model for the Wind

In this study, we use the wind model presented by Weber and Davis (1967) which is the steady flow in the equatorial plane and has a velocity

$$\vec{v} = (v_r, 0, v_\phi) \quad (13)$$

and a magnetic field

$$\vec{B} = (B_r, 0, B_\phi). \quad (14)$$

We also assume that the system is symmetric with respect to the equatorial plane. In this case, Eq. (3) becomes

$$v_r \frac{dv_r}{dr} = -\frac{1}{\rho} \frac{dP}{dr} - \frac{GM}{r^2} + \frac{v_\phi^2}{r} - \frac{B_\phi}{4\pi\rho r} \frac{\partial}{\partial r}(rB_\phi). \quad (15)$$

Conservation of mass becomes

$$\rho v_r r^2 = f = \text{const.} \quad (16)$$

The equation of the evolution of material energy becomes

$$\dot{q} = v_r \left(\frac{\partial \epsilon}{\partial r} - \frac{P}{\rho^2} \frac{\partial \rho}{\partial r} \right). \quad (17)$$

Furthermore, since $\text{div } \vec{B} = 0$,

$$r^2 B_r = \Phi = \text{const.} \quad (18)$$

We also obtain from $(\text{rot } \vec{E})_\phi = 0$ and Maxwell equation that

$$r(v_r B_\phi - v_\phi B_r) = -\Omega r^2 B_r, \quad (19)$$

where Ω is the angular velocity of the surface of the proto-neutron star. From the steady-state ϕ -equation of motion,

$$r v_\phi - \frac{B_r}{4\pi\rho v_r} r B_\phi = L = \text{const.} \quad (20)$$

These equations in this subsection represent the steady neutrino-driven wind with proper magnetic fields in the equatorial plane that has ϕ -symmetry. See detail Weber and Davis (1967).

2.3. Boundary Conditions

In this study, the surface of the proto-neutron star is considered as the inner boundary. The inner boundary conditions are composed of density, luminosities of neutrinos, mass and radius of the proto-neutron star, velocity of the outflow, angular velocity, and strength of B_r at the surface of the proto-neutron star. Temperature and electron fraction at the time when alpha-rich freezeout takes place are determined by these parameters as (Qian and Woosley 1996)

$$T_i = 1.19 \times 10^{10} \left[1 + \frac{L_{\nu_e}}{L_{\bar{\nu}_e}} \left(\frac{\epsilon_{\nu_e, \text{MeV}}}{\epsilon_{\bar{\nu}_e, \text{MeV}}} \right)^2 \right]^{\frac{1}{6}} L_{\bar{\nu}_e, 51}^{\frac{1}{8}} R_6^{-\frac{1}{3}} \epsilon_{\bar{\nu}_e, \text{MeV}}^{\frac{1}{3}} \quad [\text{K}] \quad (21)$$

and

$$Y_e = \left(1 + \frac{L_{\bar{\nu}_e} \epsilon_{\bar{\nu}_e, \text{MeV}} - 2\Delta + 1.2\Delta^2 / \epsilon_{\bar{\nu}_e, \text{MeV}}}{L_{\nu_e} \epsilon_{\nu_e, \text{MeV}} + 2\Delta + 1.2\Delta^2 / \epsilon_{\nu_e, \text{MeV}}} \right)^{-1}, \quad (22)$$

where $L_{\nu,51}$ is the individual neutrino luminosity in 10^{51} ergs s^{-1} , $\Delta = 1.293$ MeV is the neutron-proton mass difference, and $\epsilon_{\nu, \text{MeV}}$ is a neutrino energy in MeV. We assume that the neutron star radius is equal to the neutrino sphere radius.

In this study, we assume that the luminosities of neutrinos are same (Qian and Woosley 1996; Otsuki et al. 2000). The energy of neutrinos are assumed to be 12, 22, and 34 MeV for ν_e , $\bar{\nu}_e$, and other neutrinos, respectively (Woosley et al. 1994; Qian and Woosley 1996; Otsuki et al. 2000). Surface density is assumed to be 10^{10} g cm^{-3} (Otsuki et al. 2000). In the previous works, initial velocity of the outflow is chosen so that \dot{v}_{r0} , which is the radial velocity at the surface of the proto-neutron star, becomes less than $\dot{v}_{r0, \text{crit}}$. $\dot{v}_{r0, \text{crit}}$ is the critical value for supersonic solution (Qian and Woosley 1996; Otsuki et al. 2000). In this work, we also adopt this assumption so that the flow becomes subsonic and contains no critical point. In particular, we take \dot{v}_{r0} as $\dot{v}_{r0} \sim \dot{v}_{r0, \text{crit}}$ in this study. This means that the initial velocity (velocity at the surface of the proto-neutron star) is set to be maximal one because surface density is set to be constant (10^{10} g cm^{-3}). In case we try to survey the flow that contains a transition point like a shock front, we can not use Eqs. (15)–(20). This is because these differential equations diverge and break down. In order to treat such a flow that contains a discontinuity, we have to use the Rankine-Hugoniot relation instead of these equations. We will examine such flows in the forthcoming paper. Other parameters are changed parametrically. The parameters and the name of the models are given in Table 1. We take $r = 10^9$ cm for the radius of the outer boundary (Otsuki et al. 2000). Since the radius of the Fe core is about 10^8 cm, we think the radius of the outer boundary is large enough to investigate the r-process nucleosynthesis that occurs in the hot bubble.

3. Results

Output parameters are shown in Table 2. Entropy per baryon (S), dynamical timescale (τ_{dyn}), electron fraction (Y_e), and temperature (T) at the outer boundary ($r = 10^9$ cm) are shown in the table. As long as $T \geq 0.5$ MeV, entropy per baryon in radiation dominated gas is written by

$$S/k = \frac{11\pi^2}{45} \frac{k^3}{\hbar^3 c^3} \frac{T^3}{\rho/m_N}, \quad (23)$$

where m_N is the nucleon rest mass. Even if electron-positron pairs are disappeared for $T \leq 0.5$ MeV, the entropy per baryon is conserved because the wind expands adiabatically in this region. We define the dynamical timescale to be the elapsed time for the temperature to decrease from 0.5 MeV to 0.2 MeV. This is because r-process nucleosynthesis occurs in this temperature range (Woosley et al. 1994; Takahashi et al. 1994; Qian and Woosley 1996). In the following subsections, the influences of the luminosity of neutrinos, rotation, and magnetic fields on the dynamics are discussed, respectively.

3.1. Influence of luminosity of neutrinos

In order to examine the influence of the luminosities of neutrinos on the dynamics, we focus on the results of Models 10Aa, 10Ba, and 10Ca. When the angular velocity and magnetic fields are sufficiently small, the solution have to agree with QW96. Then, the results of Models 10Aa, 10Ba, and 10Ca should be explained by the solution obtained in QW96. In QW96, the entropy per baryon at the beginning of the alpha-rich freezeout, dynamical timescale, and radial velocity at the surface of the proto-neutron star are estimated as

$$S/k \sim 235 L_{\bar{\nu}_e, 51}^{-\frac{1}{6}} \epsilon_{\bar{\nu}_e, \text{MeV}}^{-\frac{1}{3}} R_6^{-\frac{2}{3}} \left(\frac{M}{1.4 M_\odot} \right), \quad (24)$$

$$\tau_{\text{dyn}} \sim 68.4 L_{\bar{\nu}_e, 51}^{-1} \epsilon_{\bar{\nu}_e, \text{MeV}}^{-2} R_6 \left(\frac{M}{1.4 M_\odot} \right) \quad [\text{s}], \quad (25)$$

and

$$v_{r0} \sim 1.8 L_{\bar{\nu}_e, 51}^{\frac{5}{3}} \epsilon_{\bar{\nu}_e, \text{MeV}}^{\frac{10}{3}} R_6^{-\frac{1}{3}} \left(\frac{10^{10} \text{g cm}^{-3}}{\rho} \right) \left(\frac{1.4 M_\odot}{M} \right)^2 \quad [\text{cm s}^{-1}], \quad (26)$$

respectively.

From Eqs. (24)-(26) and Table 2, we can see that the dependence of the entropy per baryon, dynamical timescale, and initial velocity on the luminosity of neutrinos are well explained by these equations. We also note that these values in Table 2 are well reproduced by these equations within a factor of 2-3, which warrants the accuracy of our calculations.

3.2. Influence of rotation

The effects of rotation in this framework can be understood by comparing the results of Models 10Aa-10Ac, 10Ba-10Bd, and 10Ca-10Cd in Table 2. As is clear from the results of Models 10Ac, 10Bd, and 10Cd, in which the rotation period of the proto-neutron star is (0.5 – 1) ms, the entropy per baryon becomes lower and the dynamical timescale becomes longer as the angular velocity becomes higher. This tendency is inappropriate for the success of the r-process nucleosynthesis (see section 1).

We consider the reason for this tendency. At first, we show in Figure 1 the outflow velocity, temperature, and density as a function of r for Model 10Ba and Model 10Bd. Entropy per baryon as a function of radius (r) from the center of the proto-neutron star in these models is also shown in Figure 2. From these figures, we can see that the density in Model 10Bd is much higher than that in Model 10Ba at relatively small radius ($r \leq 5 \times 10^7$ cm), which results in the lower entropy per baryon (see also Eq. (23)). From Eq. (16), we can see that v_r does not increase so much if the density does not decrease, which is verified in Figure 2. Since τ_{dyn} becomes longer when v_r is slower in the range $T = (0.2 - 0.5)\text{MeV}$, the dynamical timescale in Model 10Bd is longer than that in Model 10Ba. This is the reason for the tendency mentioned above. All we have to do is to find the reason why the density in Model 10Bd is higher than that in Model 10Ba at small radius.

From the basic equations in subsection 2.2, the derivatives of ρ by r can be written as

$$\frac{d\rho}{dr} = \frac{\frac{2f^2}{\rho r^5} - \frac{P\dot{q}}{\epsilon v_r} - \frac{GM\rho}{r^2} + \frac{2f\Phi\Omega\rho B_\phi}{4\pi f^2 - \rho\Phi^2} + \frac{\rho v_\phi^2}{r}}{\frac{4\pi f^3\Phi(L - \Omega r^2)B_\phi}{r(4\pi f^2 - \rho\Phi^2)^2} + \frac{P}{\epsilon\rho} \left(\epsilon + \frac{P}{\rho} \right) - \frac{f^2}{\rho^2 r^4}}. \quad (27)$$

We show the absolute value (in cgs units) of the each component in Eq. (27) for Model 10Ba in Figure 3a. From this figure, we find out what component dominantly contributes to the gradients of density. To compare them, we also show those for Model 10Bd in Figure 3b. Lines (a)-(f) correspond to $2f^2/\rho r^5$, $P\dot{q}/\epsilon v_r$, $GM\rho/r^2$, $\rho v_\phi^2/r$, $P(\epsilon + P/\rho)/\epsilon\rho$, and $f^2/\rho^2 r^4$ as a function of r , respectively. Here we note that B_ϕ is set to be zero in these models. Therefore, there is no components that include B_ϕ in the figures. Line (d), which represents $\rho v_\phi^2/r$, is very important here. As can be seen from Figure 3, the density gradient in both models can be approximated by

$$\frac{d\rho}{dr} \sim \frac{-\frac{GM\rho}{r^2} + \frac{\rho v_\phi^2}{r}}{\frac{P}{\epsilon\rho} \left(\epsilon + \frac{P}{\rho} \right)}. \quad (28)$$

Since the value for $\rho v_\phi^2/r$ is larger in Model 10Bd than in Model 10Ba, the absolute value of the density gradient in Model 10Bd is smaller than in Model 10Ba. Then, the density in Model 10Bd becomes larger than that in Model 10Ba for a relatively small r because the density at the surface of the proto-neutron star is set to be 10^{10} g cm $^{-3}$ in both models. This is the reason for the tendency mentioned above.

3.3. Influence of luminosity of magnetic field

The effects of magnetic fields in this framework can be understood by considering the results of Models 10Ae, 10Bg, and 10Cf in Table 2. In Models 10Ae, 10Bg, and 10Cf, in which the strength of the magnetic field is $\sim 10^{11}$ G, we could not find a solution as a steady wind from the surface of the proto-neutron star because of the following reasons. First, we focus on the first term of the denominator in Eq. (27). It diverges when $4\pi f^2 - \rho\Phi^2$ becomes zero. When this relation is satisfied, the solution diverges. This condition can be rewritten as

$$4\pi f^2 \left[1 - 7.96 \times 10^{-8} \left(\frac{10^{10} \text{g cm}^{-3}}{\rho_0} \right)^2 \left(\frac{10^5 \text{cm s}^{-1}}{v_{r0}} \right)^2 \left(\frac{B_{r0}}{10^{12} \text{G}} \right)^2 \right] = 0, \quad (29)$$

where ρ_0 , v_{r0} , and B_{r0} are the density, radial velocity, and radial magnetic field at the surface of the proto-neutron star.

From Eq. (29), we can see that the solution does not diverge when B_{r0} is small enough (Models in this study except for Models 10Ae, 10Bg, and 10Cf). This is because the second term in Eq. (29) is small enough. In Models 10Ae, 10Bg, and 10Cf, initial velocities have to be set to be high in order to avoid the divergence. However, when the initial velocity is set to be so high that the second term in Eq. (29) becomes negligible, the solution can not satisfy the condition that the solution is subsonic. That is, v_{r0} becomes larger than $v_{r0,\text{crit}}$ and the value of the denominator of Eq. (27) becomes zero at the critical point and the solution diverges after all (see also QW96). This is the reason why a steady solution can not be obtained when the magnetic fields becomes strong enough. It is also noted that we can not set v_{r0} to be small enough to avoid the divergence resulting from Eq. (29), because the initial velocity is approximated well by Eq. (26), which is confirmed by precise numerical simulations (Qian and Woosley 1996; Sumiyoshi et al. 1999).

4. Summary and Discussion

We have studied whether the effects of rotation and magnetic fields on the neutrino-driven winds could be necessary ones for the r-process nucleosynthesis. We have studied the effects of the rotation and magnetic field using simple models which are the extensions of the solution presented by Weber and Davis (1967), because the results of a realistic numerical simulation concerning with such a topic will not be understood clearly without any analytical studies.

Although our final goal is to perform such realistic numerical simulations, this approach would be a necessary step to understand the effects of the rotation and magnetic fields on the r-process nucleosynthesis.

As a result, we found that the entropy per baryon becomes lower and the dynamical timescale becomes longer as the angular velocity becomes higher, which is a bad tendency for the success of the r-process nucleosynthesis. This is because the absolute value of the density gradient becomes smaller due to the effects of rotation and the density is kept to be high at relatively small radius ($r \leq 5 \times 10^7$ cm), which results in the lower entropy per baryon and longer dynamical timescale. As for the effects of magnetic fields, we found that a solution as a steady wind from the surface of the proto-neutron star can not be obtained when the strength of the magnetic field becomes $\geq 10^{11}$ G. This is because the density gradient diverges at the critical point, which emerges at low density region like the circumstances of neutrino-driven winds in this study as long as the amplitude of the magnetic field is large enough. As a conclusion, we have to say that it seems to be difficult to cause a successful r-process nucleosynthesis in the wind models in this study.

Since the magnetic field in normal pulsars is of order 10^{12} G (e.g., Thompson 2001), the fact that a steady wind solution can not be obtained as long as the radial component of the magnetic fields at the surface of the proto-neutron star is larger than 10^{11} G seems to mean that the models in this study may not be able to be adopted in many cases. However, our models could be used since radius of proto-neutron stars are tend to be larger than normal pulsars (e.g., Wilson 1985) and the resulting magnetic fields are weaker.

We have to emphasize that there are some assumptions in this study. So, we can not say that we have proved that a successful r-process nucleosynthesis does not occur in neutrino-driven winds in which the effects of rotation and magnetic fields are taken into consideration. For example, we assumed that the flow is subsonic and there is no critical point, which is the common assumption in the previous studies on the r-process nucleosynthesis (Qian and Woosley 1996; Otsuki et al. 2000). However, we think that we do not need to restrict the solutions in such a way, that is, there may be a transition point at which Eqs. (15)–(20) break down. In most cases, the transition point will be a shock front. It means that the flow will gain entropy at the transition point, which will be a good sense to produce the r-process nuclei. The problem whether the flow contains transition points or not depends sensitively on the initial velocity on the surface of the proto-neutron star. So our final goal is to determine physically the velocity at the surface of the proto-neutron star. It means that the v_{r0} should not be given as an input parameter. It should be an output parameter. We have to investigate the mechanism for determining the outflow velocity at the surface

of the proto-neutron star for further discussions. We also assumed that the flow is steady. We should also investigate the features of the unsteady flows, although the flow is assumed to be steady in this study. It will be investigated by numerical tests assuming a simple environment. We will perform such numerical tests in the near future.

We have assumed that the form of the wind is similar as the solution of Weber and Davis (1967) here. Of course, there will be a variety of flows in which the effects of rotation and magnetic fields are taken into consideration, including the jets (Nagataki 2001). So it will be worth while surveying physical conditions using a variety of forms of the neutrino-driven winds, because we will be able to understand more precisely and correctly the results of the realistic numerical simulations. Of course, our final goal is to perform realistic numerical simulations for the wind in a collapse-driven supernova and seek a final answer whether the rotation and magnetic fields in neutrino-driven winds are the key processes for the r-process nucleosynthesis or not.

This research has been supported in part by a Grant-in-Aid for the Center-of-Excellence (COE) Research (07CE2002) and for the Scientific Research Fund (7449, 199908802) of the Ministry of Education, Science, Sports and Culture in Japan and by Japan Society for the Promotion of Science Postdoctoral Fellowships for Research Abroad.

References

- Bethe H.A., Brown G.E. 1998, ApJ 506, 780
- Cardall C.Y., Fuller G.M. 1997, ApJL 486 L111
- Cowan J.J., Pfeiffer B., Kratz K.-L., Thielemann F.-K., Sneden C., Burles S., Tytler D., Beers T.C. 1999, ApJ 521, 194
- Freiburghaus C., Rosswog S., and Thielemann F.-K. 1999, ApJL 525, L121
- Hoffman R.D., Woosley S.E., and Qian Y.-Z. 1997, ApJ 482, 951
- Ishimaru Y. and Wanajo S. 1999, ApJL 511, L33
- Meyer B.S. 1995, ApJL 449, L55
- McWilliam A., Preston G.W., Sneden C., Searle L. 1991, AJ 109, 2757
- Nagataki S. 2001, ApJ, in press (astro-ph/0010069)
- Otsuki K., Tagoshi H., Kajino T., Wanajo S. 2000, ApJ 533, 424

Qian Y.-Z., Woosley S.E. 1996, ApJ 471, 331 (QW96)

Shapiro S.L., Teukolsky S.A. 1983 in Black Holes, White Dwarfs, and Neutron Stars (New York:John Wiley & Sons, Inc.)

Sumiyoshi K., Suzuki H., Otsuki K., Terasawa M., Yamada S. 1999, astro-ph/9912156

Takahashi K., Wittl J., Janaka H.-Th. 1994, A&A 286, 857

Thompson D.J. 2001, astro-ph/0101039

van den Bergh S., Tammann G.A. 1991, ARA&A 29, 363

van den Heuvel E., Lorimer D. 1996, MNRAS 283, L37

Weber E.J., Davis L. 1967, ApJ 148, 217

Wilson R.B. 1985, in Numerical Astrophysics, p.422, eds. Centrella J.M., LeBlanc J.M., and Bowers R.L. (Jones & Bartlett: Boston)

Wiringa R.B., Fiks U., Fabrocini A. 1988, Phys. Rev. C. 38, 1010

Woosley S.E., Wilson J.R., Mathews G.J., Hoffman R.D., and Meyer B.S. 1994, ApJ 433, 229 (WWMHM94)

Table 1. Model Names and Input Parameters.

| Model | Mass (M_{\odot}) | Radius (km) | $L_{\bar{\nu}_e}$ (10^{51} ergs s^{-1}) | v_{r0} (cm s^{-1}) | $\Omega/2\pi$ (Hz) | B_{r0} (gauss) |
|-------|-------------------------|----------------|--|----------------------------|-----------------------|---------------------|
| 10Aa | 1.4 | 10 | 3.0 | 8.30(+5) | 1.0(+1) | 0 |
| 10Ab | 1.4 | 10 | 3.0 | 8.30(+5) | 1.0(+2) | 0 |
| 10Ac | 1.4 | 10 | 3.0 | 1.10(+6) | 1.0(+3) | 0 |
| 10Ad | 1.4 | 10 | 3.0 | 8.30(+5) | 1.0(+1) | 5.0(+10) |
| 10Ae | 1.4 | 10 | 3.0 | 8.50(+5) | 1.0(+1) | 5.0(+11) |
| 10Ba | 1.4 | 10 | 1.0 | 1.24(+5) | 1.0(+1) | 0 |
| 10Bb | 1.4 | 10 | 1.0 | 1.24(+5) | 1.0(+2) | 0 |
| 10Bc | 1.4 | 10 | 1.0 | 1.66(+5) | 1.0(+3) | 0 |
| 10Bd | 1.4 | 10 | 1.0 | 6.30(+5) | 2.0(+3) | 0 |
| 10Be | 1.4 | 10 | 1.0 | 1.24(+5) | 1.0(+1) | 1.1(+11) |
| 10Bf | 1.4 | 10 | 1.0 | 1.25(+5) | 1.0(+1) | 1.2(+11) |
| 10Bg | 1.4 | 10 | 1.0 | 1.20(+5) | 1.0(+1) | 1.3(+11) |
| 10Ca | 1.4 | 10 | 0.6 | 5.20(+4) | 1.0(+1) | 0 |
| 10Cb | 1.4 | 10 | 0.6 | 5.20(+4) | 1.0(+2) | 0 |
| 10Cc | 1.4 | 10 | 0.6 | 7.00(+4) | 1.0(+3) | 0 |
| 10Cd | 1.4 | 10 | 0.6 | 2.70(+5) | 2.0(+3) | 0 |
| 10Ce | 1.4 | 10 | 0.6 | 5.20(+4) | 1.0(+1) | 5.0(+10) |
| 10Cf | 1.4 | 10 | 0.6 | 1.00(+4) | 1.0(+1) | 6.0(+10) |

Model names and input parameters. Mass and radius of the proto-neutron star, luminosity of the anti-electron neutrino, radial and angular velocity, and radial component of the magnetic field at the surface of the proto-neutron star, respectively.

Table 2. Model Names and Output Parameters.

| Model | S (k) | τ_{dyn} (s) | Y_e | T_b MeV |
|-------|----------------|----------------------------|-------|--------------|
| 10Aa | 82 | 2.2(-2) | 0.43 | 6.4(-2) |
| 10Ab | 83 | 2.8(-2) | 0.43 | 7.6(-2) |
| 10Ac | 75 | 5.0(-2) | 0.43 | 9.8(-2) |
| 10Ad | 82 | 2.2(-2) | 0.43 | 6.4(-2) |
| 10Ae | — | — | 0.43 | — |
| 10Ba | 99 | 5.5(-2) | 0.43 | 4.7(-2) |
| 10Bb | 99 | 5.5(-2) | 0.43 | 4.4(-2) |
| 10Bc | 88 | 5.5(-2) | 0.43 | 3.6(-2) |
| 10Bd | 53 | 7.7(-2) | 0.43 | 2.2(-2) |
| 10Be | 99 | 5.5(-2) | 0.43 | 4.7(-2) |
| 10Bf | 97 | 3.9(-2) | 0.43 | 2.0(-2) |
| 10Bg | — | — | 0.43 | — |
| 10Ca | 107 | 8.7(-2) | 0.43 | 4.1(-2) |
| 10Cb | 108 | 9.9(-2) | 0.43 | 5.1(-2) |
| 10Cc | 94 | 6.9(-2) | 0.43 | 1.2(-2) |
| 10Cd | 58 | 1.2(-1) | 0.43 | 1.5(-2) |
| 10Ce | 107 | 8.7(-2) | 0.43 | 4.1(-2) |
| 10Cf | — | — | 0.43 | — |

Name and output parameters of Models. Entropy per baryon, dynamical timescale (τ_{dyn}), electron fraction, temperature at the outer boundary are shown respectively. The reason why physical quanta are not written in some models is that steady solutions can not be obtained in these models.

Figure Captions

Fig. 1. Outflow velocity, temperature, and density as a function of radius (r) from the center of the proto-neutron star. These values are written in unit of 10^7 cm s $^{-1}$, 1 MeV, and 10^8 g cm $^{-3}$, respectively. Solid lines correspond to Model 10Ba, whereas dashed lines correspond to Model 10Bd.

Fig. 2. Entropy per baryon as a function of radius (r) from the center of the proto-neutron star. Solid line corresponds to that of Model 10Ba. Dashed line corresponds to that of Model 10Bd.

Fig. 3. Upper panel: absolute value (in cgs units) of the each component of Eq. (27) for Model 10Ba. Lines (a)-(f) correspond to $2f^2/\rho r^5$, $P\dot{q}/\epsilon v_r$, $GM\rho/r^2$, $\rho v_\phi^2/r$, $P(\epsilon + P/\rho)/\epsilon\rho$, and $f^2 \rho^2 r^4$ as a function of r , respectively. The discontinuity of line (b) at $r \sim 10^7$ cm reflects the freezeout of the neutrino reactions (see subsection 2.1). Lower panel: same as left, but for Model 10Bd.

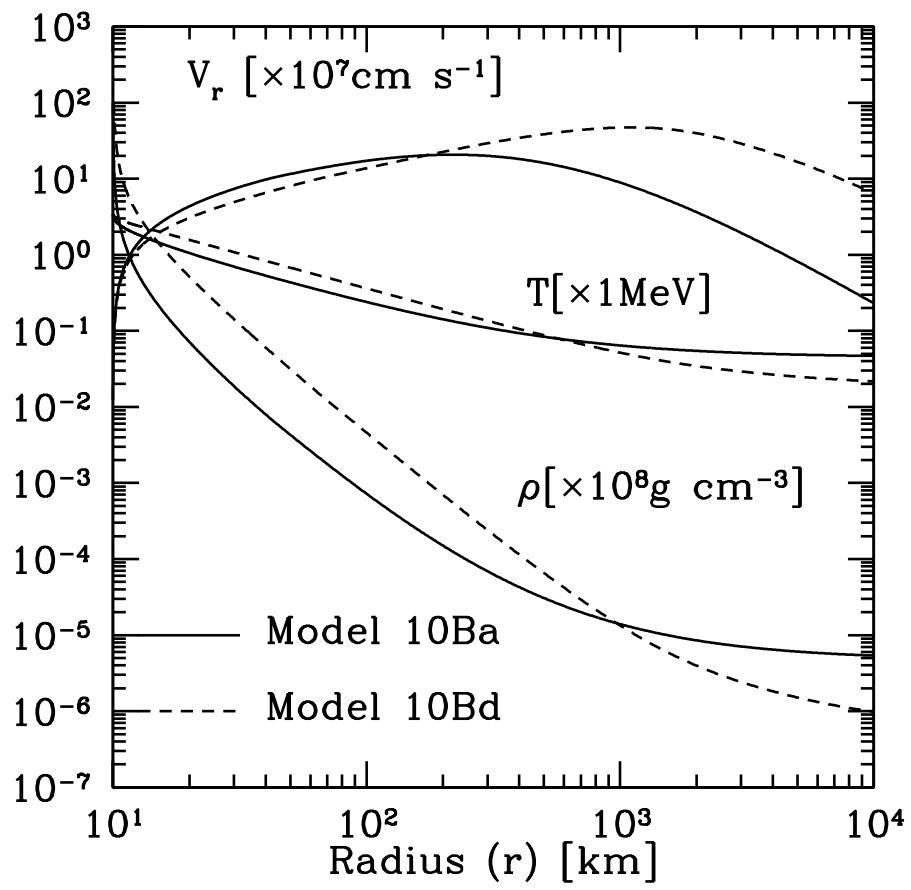


Fig. 1..

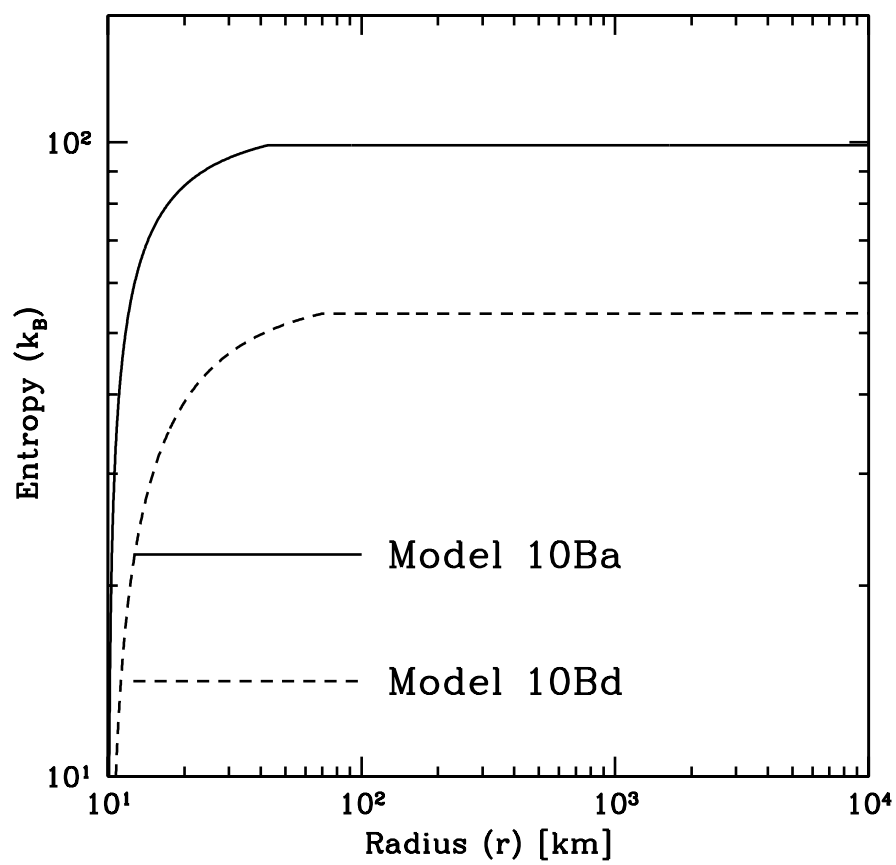


Fig. 2..

